Spectrophotometric determination of carbonate ion concentrations: Elimination of instrument-dependent offsets and calculation of in situ saturation states

Jonathan D. Sharp[a], Robert H. Byrne[a,*], Xuewu Liu[a], Richard A. Feely[b], Erin E. Cuyler[a], Rik Wanninkhof[c], and Simone R. Alin[b]

[a]College of Marine Science, University of South Florida
140 7th Avenue South, St. Petersburg, FL 33701, USA

[b]Pacific Marine Environmental Laboratory, NOAA
7600 Sand Point Way NE, Seattle, WA 98115, USA

[c]Atlantic Oceanographic and Meteorological Laboratory, NOAA
4301 Rickenbacker Causeway, Miami, FL 33149, USA

Environmental Science and Technology

Abstract

This work describes an improved algorithm for spectrophotometric determinations of seawater carbonate ion concentrations ($[CO_3^{2-}]_{spec}$) derived from observations of ultraviolet absorbance spectra in lead-enriched seawater. Quality-control assessments of $[CO_3^{2-}]_{spec}$ data obtained on two NOAA research cruises (2012 and 2016) revealed a substantial inter-cruise difference in average $\Delta[CO_3^{2-}]$ (the difference between a sample's $[CO_3^{2-}]_{spec}$ value and the corresponding $[CO_3^{2-}]$ value calculated from paired measurements of pH and dissolved inorganic carbon). Follow-up investigation determined that this discordance was due to the use of two different spectrophotometers, even though both had been properly calibrated. Here we present an essential methodological refinement to correct $[CO_3^{2-}]_{spec}$ absorbance data for small but significant instrumental differences. (This correction is not necessary for pH determinations from sulfonephthalein dye absorbances). After correcting the shipboard absorbance data, we fit the combined-cruise dataset to produce empirically updated parameters for use in processing future (and historical) $[CO_3^{2-}]_{spec}$ absorbance measurements. With the new procedure, the average $\Delta[CO_3^{2-}]$ offset between the two aforementioned cruises was reduced from 3.7 μmol kg^{-1} to 0.7 μmol kg^{-1}, which is well within the standard deviation of the measurements (1.9 μmol kg^{-1}). We also introduce an empirical model to calculate in situ carbonate ion concentrations from $[CO_3^{2-}]_{spec}$. We demonstrate that these in situ values can be used to determine calcium carbonate saturation states that are in good agreement with those determined by more laborious and expensive conventional methods.

1. Introduction

The current trend of increasing atmospheric carbon dioxide (CO_2) concentration and the dissolution of some of that CO_2 into the ocean is significantly altering seawater chemistry.[1–3] Anthropogenic CO_2 is decreasing both seawater pH and the concentration ratio of $[CO_3^{2-}]/[HCO_3^-]$ in the ocean.[4] Recognition of this phenomenon has motivated global carbon monitoring studies[5] and numerous regional efforts[6–11] intended to enhance our understanding of the marine CO_2 system.

The marine CO_2 system is commonly examined by directly determining two or more of the four primary CO_2 system measurement parameters: pH, total dissolved inorganic carbon (C_T), total alkalinity (A_T), and CO_2 fugacity (f_{CO2}). Any two of these parameters can be used with thermodynamic CO_2 system models to calculate all remaining system parameters, including carbonate ion concentrations ($[CO_3^{2-}]$).[12]

Of the four dissolved CO_2 species in seawater ($CO_{2(aq)}$, H_2CO_3, HCO_3^-, and CO_3^{2-}), carbonate ions are of particular importance due to their control over calcium carbonate ($CaCO_3$) saturation states (Ω). Saturation states regulate calcification rates of marine calcifying organisms,[13–18] water column dissolution rates of solid $CaCO_3$ (e.g., calcite, aragonite),[19,20] and preservation of solid $CaCO_3$ in sediments.[21,22] All of these processes are critical components of both local and global carbon budgets.

Recent development of a method to determine total carbonate ion concentrations in seawater ($[CO_3^{2-}]_{spec}$) through spectrophotometric observations of lead equilibria has added carbonate as a fifth measurable CO_2 system parameter.[23] Several studies have demonstrated the efficacy of this method.[24–26] Determinations of $[CO_3^{2-}]_{spec}$ are

advantageous because they are rapid, simple, and inexpensive; they are also amenable to adaption for in situ analyses.

In this paper, we identify a methodological artifact that creates incongruent $[CO_3^{2-}]_{spec}$ values for absorbance measurements made with different spectrophotometers. We describe this artifact and its consequences, as well as an essential methodological refinement to avoid such problems in the future (and to correct past occurrences). The refined protocol includes instrument-specific assessments of wavelength calibration offsets and a new computational algorithm for calculating $[CO_3^{2-}]_{spec}$ from offset-corrected absorbance measurements. Additionally, we present a model for calculating in situ $CaCO_3$ saturation states directly from shipboard measurements of $[CO_3^{2-}]_{spec}$. The datasets used in this study include 2,681 corresponding observations of Pb(II) absorbance spectra, salinity, C_T, and pH obtained on two NOAA research cruises in 2012 and 2016.

1.1. Theory

The absorbance ($_\lambda A$) of Pb(II) in seawater at a given wavelength (λ) is described by the following equation:[27,28]

$$\frac{{}_\lambda A}{l \cdot [Pb]_T} = \frac{{}_\lambda\varepsilon_{Pb} + {}_\lambda\varepsilon_{PbCO_3} \cdot {}_{CO_3}\beta_1 \cdot [CO_3^{2-}]}{1 + {}_{CO_3}\beta_1 \cdot [CO_3^{2-}]} \quad (1)$$

where l is the pathlength of the spectrophotometer cell and $[Pb]_T$ is the total lead concentration. The term ${}_\lambda\varepsilon_{PbCO_3}$ represents the molar absorptivity of $PbCO_3^0$, ${}_\lambda\varepsilon_{Pb}$ represents the absorbance per mole of Pb(II) at low pH (attributable to Pb^{2+} and lead

chloride complexes), and ${}_{CO_3}\beta_1$ is the formation constant for $PbCO_3^0$ expressed in terms of the total (free plus ion-paired) carbonate ion concentration ($[CO_3^{2-}]$). All carbonate ion concentrations in this paper are expressed as total concentrations.

The complexation of lead and carbonate is represented by

$$Pb^{2+} + CO_3^{2-} \rightleftharpoons PbCO_3^0 \quad (2)$$

and the formation constant for $PbCO_3^0$ is defined as

$${}_{CO_3}\beta_1 = \frac{[PbCO_3^0]}{[Pb^{2+}]_T[CO_3^{2-}]} \quad (3)$$

where $[PbCO_3^0]$ is the concentration of dissolved $PbCO_3^0$ (including minor contributions from $PbCO_3Cl^-$) and $[Pb^{2+}]_T$ is the sum concentration of free lead and lead chloride complexes.

Using eq 1, the absorbance ratio of Pb(II) in seawater measured at wavelengths of 234 and 250 nanometers (nm)[23] is given as

$$R = \frac{{}_{250}A}{{}_{234}A} = \frac{{}_{250}\varepsilon_{Pb} + {}_{250}\varepsilon_{PbCO_3} \cdot {}_{CO_3}\beta_1 \cdot [CO_3^{2-}]}{{}_{234}\varepsilon_{Pb} + {}_{234}\varepsilon_{PbCO_3} \cdot {}_{CO_3}\beta_1 \cdot [CO_3^{2-}]} \quad (4)$$

Eq 4 can be rearranged[23] to provide an equation that allows for determination of $[CO_3^{2-}]$ (i.e., $[CO_3^{2-}]_{spec}$) in terms of the ratio (R) of Pb(II) absorbances at 234 and 250 nm in lead-enriched seawater:

$$-\log[CO_3^{2-}]_{spec} = \log\{{}_{CO_3}\beta_1/e_2\} + \log\{(R - e_1)/(1 - R \cdot e_3/e_2)\} \quad (5)$$

where e_1, e_2, and e_3/e_2 are salinity-dependent molar absorbance ratios defined as

$$e_1 = \frac{{}_{250}\varepsilon_{PbCO_3}}{{}_{234}\varepsilon_{PbCO_3}}, e_2 = \frac{{}_{250}\varepsilon_{Pb}}{{}_{234}\varepsilon_{PbCO_3}}, e_3/e_2 = \frac{{}_{234}\varepsilon_{Pb}}{{}_{250}\varepsilon_{Pb}} \quad (6)$$

Absorbances at 350 nm, a non-absorbing wavelength, are also recorded for correction of baseline absorbance changes caused by variations in cell positioning, lamp intensity, etc. Baseline-corrected absorbance ratios are calculated as

$$R = \frac{{}_{250}A - {}_{350}A}{{}_{234}A - {}_{350}A} \quad (7)$$

where ${}_{350}A$ is the absorbance measurement at 350 nm relative to the original baseline (seawater-only) measurement at the same wavelength.

Eq 5, which is parallel in form to the equation used to determine seawater pH on the total scale (pH_T) from sulfonephthalein absorbance ratios,[29,30] allows for convenient calculation of $[CO_3^{2-}]_{spec}$ with a minimal number of parameters. The $\log\{{}_{CO_3}\beta_1/e_2\}$, e_1, and e_3/e_2 terms have been previously determined through laboratory experiments and empirical fitting of field data.[23–25] The most recent characterization of these terms as quadratic functions of salinity at 25 °C is presented in Patsavas et al.[25]

2. Methods

2.1. Research cruises

The 2012 NOAA Gulf of Mexico and East Coast Carbon Cruise (GOMECC-2) was carried out between July 21 and August 13 on the NOAA Ship *Ronald H. Brown*.[31] A total of 93 stations across 8 transects in the Gulf of Mexico and off the East Coast of the United States were sampled from surface to seafloor (Figure S1). Hydrographic data (salinity, temperature, and depth) were measured with a rosette-mounted CTD (SBE 9*plus*, Sea-Bird Scientific). Measured chemical parameters included pH_T, $[CO_3^{2-}]_{spec}$, C_T, A_T, f_{CO2}, dissolved oxygen, and nutrients. All CO_2 system parameters except $[CO_3^{2-}]_{spec}$ were determined using the standard operating protocols detailed in Dickson et al.[12] Purified *m*-cresol purple was used for spectrophotometric pH_T measurements.[30] Coulometry was used to measure C_T.[32] A total of 1,216 $[CO_3^{2-}]_{spec}$ measurements were made, and a total of 1,077 conjugate measurements of $[CO_3^{2-}]_{spec}$, pH_T, and C_T were available for comparison.

The 2016 NOAA West Coast Ocean Acidification Cruise (WCOA 2016) was carried out between May 5 and June 7 on the NOAA Ship *Ronald H. Brown*. A total of 135 stations across 16 transects between central Baja California (~25°N) and waters north of Vancouver Island (~52°N) were sampled from surface to seafloor (Figure S1). Procedures to collect hydrographic and chemical data were identical to those used on the GOMECC-2 cruise. A total of 1,761 $[CO_3^{2-}]_{spec}$ measurements were made, and a total of 1,604 conjugate measurements of $[CO_3^{2-}]_{spec}$, pH_T, and C_T were available for comparison.

2.2. $[CO_3^{2-}]_{spec}$ measurement procedures

On both cruises, carbonate ion concentrations were measured according to the procedures outlined in Patsavas et al.[25] Seawater samples were collected directly from Niskin bottles into quartz optical cells, which were immediately sealed with Teflon™ caps, then thermostatted to 25 °C (±0.01 °C). For each cell, a baseline (seawater-only) measurement was followed by a 20 μL addition of 22 mM lead perchlorate ($Pb(ClO_4)_2$) solution. Five spectra were recorded for each sample of lead-enriched seawater, and absorbance values at 234, 250, and 350 nm were recorded and averaged. An absorbance ratio (eq 7) was calculated for each sample. Absorbance measurements were made using Agilent 8453 UV-visible spectrophotometers (Agilent Technologies) — the same model but different instruments on the two cruises.

2.3. Initial evaluation of cruise data

Measured $[CO_3^{2-}]_{spec}$ values were determined using eq 5 with measured absorbance ratios (R) and the perturbation correction and salinity-dependent parameters from eqs 12–15 in Patsavas et al.[25]

For comparison to these shipboard $[CO_3^{2-}]_{spec}$ measurements, paired measurements of pH_T and C_T were used to calculate $[CO_3^{2-}]_{pH,C_T}$ values for the same samples. Version 2.1 of the CO2SYS Microsoft Excel program[33] was used for all CO_2 system calculations in this paper, with the dissociation constants of Lueker et al.,[34] the K_{HSO4} formulation of Dickson et al.,[35] and the total boron to salinity ratio of Lee et al.[36] Uncertainty in the resulting $[CO_3^{2-}]_{pH,C_T}$ dataset is approximately 2 μmol kg^{-1}.

For our analyses, archived data that were flagged 4 (bad) according to WOCE quality control standards[37] were excluded. Data flagged 2 (acceptable), 3 (questionable), or 6 (duplicate) were included. While, the distinction between "acceptable" and "questionable" measurements is largely at the discretion of the investigator,[37] this practice ensured that all measurements explicitly flagged as "bad" were excluded from our analyses.

Residual (Δ) values were determined for each sample: $\Delta\left[CO_3^{2-}\right] = [CO_3^{2-}]_{pH,C_T} - [CO_3^{2-}]_{spec}$. For each dataset, outliers were eliminated by deleting $\Delta[CO_3^{2-}]$ values that were more than three standard deviations from the mean $\Delta[CO_3^{2-}]$ value (1.4% of the data points were eliminated).

2.4. Determination of spectrophotometer wavelength offsets

The wavelength calibrations of five Agilent 8453 UV-visible spectrophotometers — all of which had been previously calibrated according to manufacturer's instructions and some of which had been used on recent research cruises — were assessed using SRM 2034,[38] a National Institute of Standards and Technology (NIST) holmium oxide wavelength standard. Dilute holmium oxide solution exhibits several distinct absorbance peaks between 240 and 650 nm. Using signal averaging, Agilent 8453 spectrophotometers can locate the positions of these peaks to the hundredth of a nanometer. The instrument-specific wavelength offset ($\Delta\lambda_{241.1}$) is defined as the difference between the standard wavelength of the second holmium oxide absorbance peak as specified by NIST (λ = 241.10 nm) and the wavelength at which the spectrophotometer reports that peak.

2.5. Development of wavelength offset correction equation

The measured wavelength offsets of the five spectrophotometers were used to develop an equation to correct measured absorbance ratios (R) for instrument-specific wavelength offsets. Four seawater batches with distinct carbonate ion concentrations (~130 to 250 μmol kg^{-1}) were examined. Triplicate samples from each batch were analyzed on each spectrophotometer, according to the procedure detailed in Section 2.2, and the average R of each triplicate set was calculated.

This R dataset was then used to determine, for each seawater batch, the theoretical absorbance ratio, R^0, that would have been observed on a "perfectly calibrated" instrument (i.e., one with a wavelength offset of 0 nm). For each batch, a linear least squares regression was performed using the five R values (one from each spectrophotometer) and the five values of $\Delta\lambda_{241.1}$. The y-intercepts of the resulting regression equations yielded four batch-specific values of R^0.

Finally, differences between the 20 values of R and R^0 (ΔR) were computed and plotted against $\Delta\lambda_{241.1}$. A linear regression through the data yielded an equation for absorbance ratio corrections as a function of wavelength offset.

2.6. Refinement of $[CO_3^{2-}]_{spec}$ computational algorithm

After characterizing the GOMECC-2 and WCOA 2016 spectrophotometers (Section 2.4) and using the wavelength correction equation (Section 2.5) to obtain offset-corrected absorbance ratios (R^0) from the 2,681 shipboard absorbance measurements, we used the offset-corrected dataset to generate a revised set of parameterizations for the $[CO_3^{2-}]_{spec}$

computational algorithm. Eq 5 was fitted to $[CO_3^{2-}]_{pH,C_T}$ values, using R^0 values in place of R and second-order salinity-dependent polynomials for $\log\{_{CO_3}\beta_1/e_2\}$, e_1, and e_3/e_2 (SigmaPlot software). The fitting procedure, which was similar to that of Easley et al.,[24] yielded a set of empirically defined parameters that can be used with a modification of eq 5 in order to determine $[CO_3^{2-}]_{spec}$ from offset-corrected ultraviolet absorbance ratios (R^0):

$$-\log[CO_3^{2-}]_{spec} = \log\{_{CO_3}\beta_1/e_2\} + \log\{(R^0 - e_1)/(1 - R^0 \cdot e_3/e_2)\} \quad (8)$$

2.7. Method to verify fitting procedure

To verify that this fitting procedure generated parameters that can adequately describe an independent dataset, the combined GOMECC-2 and WCOA 2016 dataset was randomly divided into two groups. One group of R^0 values was used to obtain provisional characterizations of the $\log\{_{CO_3}\beta_1/e_2\}$, e_1, and e_3/e_2 parameters, according to the empirical fitting procedure described above. The other group of R^0 values was then processed with eq 8, using these provisional parameters, to obtain $[CO_3^{2-}]_{spec}$ values. The resulting $[CO_3^{2-}]_{spec}$ values were compared with $[CO_3^{2-}]_{pH,C_T}$ values for the same samples.

2.8. Development of a model to calculate in situ $[CO_3^{2-}]^*_{spec}$ from $[CO_3^{2-}]_{spec}$

An empirical model was developed to calculate values of $[CO_3^{2-}]^*_{spec}$ (carbonate ion concentrations at in situ temperature, t, and pressure, P) from values of $[CO_3^{2-}]_{spec}$ (determined at laboratory conditions of 25 °C and 1 atm total pressure). The resulting

$[CO_3^{2-}]^*_{spec}$ values allow for the calculation of in situ $CaCO_3$ saturation states and thus, if the available data cover an adequate geographic extent, the mapping of saturation horizons. The form of the model is based upon similar empirical models that have been presented for in situ pH calculations:[39,40]

$$[CO_3^{2-}]^*_{spec} = [CO_3^{2-}]_{spec} + A + Bt + Ct^2 \quad (9)$$

where t is temperature in (°C) and A, B, and C are functions of S, P, and $[CO_3^{2-}]_{spec}$.

To generate a synthetic dataset to determine the empirical parameters A, B, and C, 462 pairs of fixed A_T (2088 to 2564 μmol kg^{-1}) and C_T (1740 to 2564 μmol kg^{-1}) values spanning a range of A_T/C_T ratios (1.0 to 1.2) were input to CO2SYS Version 2.1[33] over specified ranges of temperature, salinity, and pressure (t = 0 to 40 °C, S = 20 to 40, and P = 0 to 2500 dbars). For each input condition, a value of $\left[CO_3^{2-}\right]$ at 25 °C and 0 dbars (analogous to $[CO_3^{2-}]_{spec}$) was calculated, along with a corresponding value of $\left[CO_3^{2-}\right]$ at in situ t and P (analogous to $[CO_3^{2-}]^*_{spec}$). Silicate and phosphate concentrations were omitted as the effect they have on the difference between in situ and ex situ $\left[CO_3^{2-}\right]$ is negligible. The resulting synthetic dataset contained a total of 492,492 unique conditions. Using a least-squares fitting routine (SigmaPlot software), the calculated values of in situ $[CO_3^{2-}]^*_{spec}$ were modeled (eq 9) as a function of t, S, P, and $[CO_3^{2-}]_{spec}$.

2.9. Calculation of spectrophotometric in situ aragonite saturation states

The resulting $[CO_3^{2-}]^*_{spec}$ model (eq 9) was applied to the 2012 and 2016 field measurements of $[CO_3^{2-}]_{spec}$ to calculate in situ aragonite saturation states (Ω_A), here termed $\Omega_{A(spec)}$:

$$\Omega_{A(spec)} = \frac{[Ca^{2+}]_T [CO_3^{2-}]^*_{spec}}{K'_{sp_A}} \quad (10)$$

where $[Ca^{2+}]_T$ is the total calcium ion concentration, $[CO_3^{2-}]^*_{spec}$ is the in situ total carbonate ion concentration (free plus ion-paired), and K'_{sp_A} is the apparent thermodynamic solubility product for aragonite ($K'_{sp_A} = [Ca^{2+}]_T [CO_3^{2-}]^*_{sat}$, where $[CO_3^{2-}]^*_{sat}$ is carbonate concentration at saturation). $[Ca^{2+}]_T$ was estimated from salinity measurements ($[Ca^{2+}]_T = 0.0102821 \cdot S/35$),[41] and K'_{sp_A} was determined using the equations of Mucci[42] with the pressure correction of Millero.[39]

The resulting spectrophotometric in situ aragonite saturation states were compared to in situ saturation states calculated from paired shipboard measurements of pH_T and C_T, here termed $\Omega_{A(pH,C_T)}$.

3. Results and Discussion

3.1. Initial assessment of $[CO_3^{2-}]_{spec}$ cruise data, 2012 and 2016

Systematic differences in $\Delta[CO_3^{2-}]$ values (on average, 3.7 μmol kg^{-1}) between the GOMECC-2 and WCOA 2016 cruises (Figure 1) are apparent when absorbance measurements are processed using the algorithm from Patsavas et al.[25] The overall average

$\Delta[CO_3^{2-}]$ of the combined-cruise dataset is –2.78 ± 2.9 μmol kg^{-1}. The $\Delta[CO_3^{2-}]$ values for the GOMECC-2 dataset are reasonably scattered about zero because the Patsavas algorithm was empirically optimized using the (uncorrected) GOMECC-2 data. Results described in the following sections demonstrate that the $\Delta[CO_3^{2-}]$ differences shown in Figure 1 are due to the use of different spectrophotometers (with different wavelength offsets) on the two cruises.

3.2. Spectrophotometer wavelength offsets

For the spectrophotometer characterizations, 241.10 nm was chosen to be the wavelength of focus because (a) it lies between the $[CO_3^{2-}]_{spec}$ measurement wavelengths of 234 and 250 nm and (b) SRM 2034 shows an especially sharp absorbance peak at 241.10 nm.[38] Figure 2 describes conceptually how sub-nanometer wavelength offsets lead to errors in measured Pb(II) absorbance ratios.

The wavelength offsets ($\Delta\lambda_{241.1}$) of the five wavelength-calibrated spectrophotometers examined in this work were 0.01 nm, –0.04 nm, –0.26 nm, 0.21 nm, and –0.03 nm. The specified wavelength accuracy limit for Agilent 8453 spectrophotometers is ±0.5 nm. All of the spectrophotometers were well within this limit.

The three "Uncorrected Data" columns of Table 1 show absorbance ratios (R) measured for the four different seawater batches on the five different spectrophotometers; the resulting values of $[CO_3^{2-}]_{spec}$, calculated using eq 5 and the algorithm of Patsavas et al.;[25] and the resulting residuals (i.e., $[CO_3^{2-}]_{spec}$ minus the mean $[CO_3^{2-}]_{spec}$ value for the given seawater batch). The $[CO_3^{2-}]_{spec}$ residuals, which range from –16.75 to 13.69 μmol kg^{-}

[1], are consistently largest in magnitude for the spectrophotometers with the largest wavelength offsets.

3.3. Wavelength offset correction equation

Figure 3a illustrates how the R data of Table 1 were used to obtain, for each seawater batch, the absorbance ratio that would have been measured by a "perfectly calibrated" spectrophotometer, as defined in Section 2.5 (i.e., R^0). This example, from seawater batch #2, is representative of the other three batches as well.

Figure 3b shows ΔR values ($R - R^0$) plotted as a function of wavelength offset ($\Delta\lambda_{241.1}$). Linear regression of these data yielded an empirical relationship that can be used to convert R values determined on any wavelength-calibrated spectrophotometer to offset-corrected values of R^0:

$$R^0 = R - 0.0265 \cdot \Delta\lambda_{241.1} \quad (11)$$

The three "Corrected Data" columns of Table 1 show the corrected absorbance ratios thus obtained (R^0); the resulting values of $[CO_3^{2-}]_{spec}$, calculated using eq 8 and the algorithm of Patsavas et al.;[25] and the resulting $[CO_3^{2-}]_{spec}$ residuals.

Comparison of the corrected and uncorrected data shows that the R^0 values exhibit far less variation among instruments than do the original R values. Similarly, the $[CO_3^{2-}]_{spec}$ residuals for the corrected data show no anomalously large values such as those seen in the residuals of the uncorrected data. Indeed, in terms of carbonate ion concentrations, the

corrected data show an average (per batch) standard deviation of 2.01 μmol kg^{-1} compared to 7.40 μmol kg^{-1} for the uncorrected data.

These observations demonstrate that for the types of UV-visible spectrophotometers often used for shipboard and laboratory work (Agilent 8453 instruments, in this case), the accuracy necessary for $[CO_3^{2-}]_{spec}$ measurements is not achieved using the wavelength recalibration procedure[43] recommended by the manufacturer. Offsets well within the specified wavelength accuracy limit (±0.5 nm, in this case) can lead to considerable inconsistencies in measured $[CO_3^{2-}]_{spec}$. For example, the 0.5 nm offset shown in Figure 2 corresponds to a 10% difference in $[CO_3^{2-}]_{spec}$. Wavelength offsets for instruments provided by other manufacturers likely have similar implications.

The proposed wavelength offset correction (eq 11), which is based on the NIST standard SRM 2034, is an effective way to remedy the problem. Repeated evaluations with SRM 2034 have indicated that the wavelength offset for a given instrument remains quite constant over time (provided the instrument is not recalibrated in the interim).

It is important to note that the sub-nanometer wavelength offsets described in this paper are not detrimental to spectrophotometric pH_T measurements obtained from sulfonephthalein absorbance ratios. The wavelengths used for pH_T measurements are located at the crests of absorbance peaks,[29,30,44] where small discrepancies in wavelength calibration have no observable effect on measured absorbance ratios.

3.4. Refined $[CO_3^{2-}]_{spec}$ computational algorithm

The salinity-dependent parameters obtained through the empirical fitting procedure described in Section 2.6 are:

$$\log\{{}_{CO_3}\beta_1/e_2\} = 6.87057 - 0.142142 \cdot S + 0.00190892 \cdot S^2 \quad (12)$$

$$e_1 = 0.787458 - 0.0339648 \cdot S + 0.000583574 \cdot S^2 \quad (13)$$

$$e_3/e_2 = 2.52288 - 0.0383205 \cdot S \quad (14)$$

A quadratic term in the e_3/e_2 parameter, which was reported in previous publications,[23–25] proved to be insignificant in this context and was therefore dropped. To obtain a spectrophotometric carbonate ion concentration for a seawater sample, these parameters are to be used in eq 8, which relates $[CO_3^{2-}]_{spec}$ to offset-corrected absorbance ratios (R^0).

Values of $\Delta[CO_3^{2-}]$ for the GOMECC-2 and WCOA 2016 cruises, determined using eqs 11 and 8 (with the parameters of eqs 12–14), are displayed in Figure 4. Outliers were again eliminated by deleting $\Delta[CO_3^{2-}]$ values that were more than three standard deviations from the mean (1.3% of the data points were eliminated). The combined correction procedure and new computational algorithm produce concordant $[CO_3^{2-}]_{spec}$ results obtained using different instruments on different cruises. The average value of $\Delta[CO_3^{2-}]$ was –0.03 ± 1.9 μmol kg^{-1}, and the average difference in $\Delta[CO_3^{2-}]$ between the two cruises was 0.7 μmol kg^{-}

[1]. This comparison represents a substantial improvement over the results obtained using the Patsavas et al.[25] algorithm with uncorrected *R* values (Figure 1).

The relative standard uncertainty of the $[CO_3^{2-}]_{spec}$ measurements was 1.5%. In the context of the measurement quality goals of the Global Ocean Acidification Observing Network (GOA-ON), this result is well within the weather objective, which "requires the carbonate ion concentration…to have a relative standard uncertainty of 10%".[45] It also very nearly meets the climate objective, which "requires that a change in the carbonate ion concentration be estimated at a particular site with a relative standard uncertainty of 1%".[45] It is encouraging that, at present, spectrophotometric measurements of carbonate ion concentrations can nearly achieve GOA-ON's climate objective, even when the data used to assess concentration changes are collected using different instruments and operators.

3.5. Verification of fitting procedure

The parameters described in eqs 12–14 (obtained by fitting the entire combined-cruise dataset) can be considered as optimal for computation of $[CO_3^{2-}]_{spec}$ from corrected absorbance measurements. As a demonstration of the efficacy of this fitting procedure, an additional assessment (Section 2.7) was undertaken by processing one half of the cruise data, using $\log\{_{CO_3}\beta_1/e_2\}$, e_1, and e_3/e_2 parameters that were generated by fitting the other half of the data. The resulting average $\Delta[CO_3^{2-}]$ was –0.10 ± 2.1 μmol kg^{-1}. This result compares favorably with the average $\Delta[CO_3^{2-}]$ obtained by parameterizing the entire combined-cruise dataset to obtain eqs 12–14 (–0.03 ± 1.9 μmol kg^{-1}).

3.6. Model to calculate in situ $[CO_3^{2-}]^*_{spec}$ from $[CO_3^{2-}]_{spec}$

The fitting procedure described in Section 2.8 provided an empirical relationship between in situ carbonate ion concentrations ($[CO_3^{2-}]^*_{spec}$) and carbonate ion concentrations measured under laboratory conditions ($[CO_3^{2-}]_{spec}$). The parameters *A*, *B,* and *C* in eq 9 have the following dependencies on *S*, *P* (dbars), and $[CO_3^{2-}]_{spec}$ (here expressed in µmol kg^{-1}):

$$10^2 \cdot A = 296.280 - 28.6065 \cdot S - 23.2553 \cdot (P/100) - 2.81230 \cdot \left[CO_3^{2-}\right]_{spec} \quad (15)$$

$$10^3 \cdot B = -54.2813 + 6.50835 \cdot S + 3.68097 \cdot (P/100) + 1.94542 \cdot \left[CO_3^{2-}\right]_{spec} \quad (16)$$

$$10^4 \cdot C = 8.20538 + 1.63374 \cdot S - 0.375824 \cdot (P/100) - 0.504280 \cdot \left[CO_3^{2-}\right]_{spec} \quad (17)$$

According to eq 9, carbonate ion concentration increases with increasing temperature by somewhat more than 0.4 µmol kg^{-1} per °C. With increasing pressure, carbonate ion concentration decreases by somewhat less than 0.2 µmol kg^{-1} per 100 dbars. For the range of data considered in the model, the differences between in situ carbonate concentrations calculated using (a) coupled values of A_T and C_T versus (b) eq 9 and eqs 15–17 with a theoretical $[CO_3^{2-}]_{spec}$ value showed a standard deviation of ±0.51 µmol kg^{-1}.

3.7. Evaluation of $[CO_3^{2-}]_{spec}$-based in situ aragonite saturation states

Using the field data, it was possible to compare two independent characterizations of aragonite saturation state: $\Omega_{A(pH,C_T)}$ versus $\Omega_{A(spec)}$. Differences between the two are shown as a function of measured $[CO_3^{2-}]^*_{spec}$ in Figure 5. The average difference is –0.0007 ± 0.022 for the WCOA 2016 cruise and 0.0011 ± 0.041 for the GOMECC-2 cruise.

Representative cross sections of $\Omega_{A(pH,C_T)}$ and $\Omega_{A(spec)}$ are shown in the top two panels of Figure 6, and a cross-section of their differences is shown in the bottom panel. Saturation states computed using the new model agree well with those calculated from paired measurements of C_T and pH_T, especially in surface waters where saturation states can significantly alter the life cycles of calcareous organisms.

Overall, the relative standard uncertainty of the $\Omega_{A(spec)}$ calculations is less than 2%. Again, this result can be viewed in the context of GOA-ON's measurement quality goals.[45] GOA-ON presents relative standard uncertainty goals for $[CO_3^{2-}]$ (10% for weather, 1% for climate), which closely correspond to relative standard uncertainties in Ω. Similar to the $[CO_3^{2-}]_{spec}$ result, the relative standard uncertainty of the $\Omega_{A(spec)}$ calculations is well within GOA-ON's weather objective and nearly meets the climate objective.

The closely similar saturation state depictions of Figure 6 can also be viewed in context of the cost, time, and manpower required to produce those data. Determinations of in situ $\Omega_{A(pH,C_T)}$ (top panel) require a spectrophotometer and a coulometer, with a combined per-sample analysis time of ~13 minutes (~3 minutes for pH_T and ~10 minutes for C_T), and two teams of analysts to sustain 24-hour operations at an acceptable pace. Determinations of in situ $\Omega_{A(spec)}$ (middle panel) require only a spectrophotometer, with a

per-sample analysis time of ~3 minutes, and a single team of analysts to sustain 24-hour operations at an acceptable pace.

3.8 Implications

Previous publications[23-26] have discussed the advantages of spectrophotometric determinations of seawater carbonate ion concentrations. This work builds on that earlier body of work by (a) identifying and eliminating a significant instrumental artifact and (b) extending the utility of $[CO_3^{2-}]_{spec}$ measurements to provide in situ carbonate ion concentrations and in situ $CaCO_3$ saturation states.

The laboratory spectrophotometers required to measure $[CO_3^{2-}]_{spec}$ are widely available and relatively inexpensive, unlike the specialized equipment required to measure C_T and A_T. This work, moreover, improves the quality of the data that such spectrophotometers can deliver. In addition, as noted above, measurements of $[CO_3^{2-}]_{spec}$ are, like spectrophotometric pH_T measurements, far more rapid than measurements of C_T and A_T.

A critical advantage of $[CO_3^{2-}]_{spec}$ is that it can be used as a fifth measurable CO_2 system parameter; this addition has implications for examinations of internal consistency. Measurements of $[CO_3^{2-}]_{spec}$ (like pH_T and C_T) are not biased by organic alkalinity, which can influence internal consistency when A_T is used as an input parameter.[46] Similarly, $[CO_3^{2-}]_{spec}$ can provide insight into known problems, such as the observed bias in calculated f_{CO2} that is evident at high f_{CO2} when A_T and C_T are used as input parameters.[47] The use of carbonate as a fifth reliable measurement parameter is also beneficial because of its

methodological similarity to spectrophotometric pH_T measurements. No other two CO_2 system parameters have this similarity, whereby a single type of instrumentation can be used for determinations of two parameters via measurements of absorbance ratios. This has implications for CO_2 system characterizations that are both accurate and methodologically simplistic.

Our model for calculating in situ $[CO_3^{2-}]^*_{spec}$ values and $CaCO_3$ saturation states from shipboard $[CO_3^{2-}]_{spec}$ measurements bypasses the need for labor-intensive, conjugate measurements of multiple (i.e., two or more) CO_2 system measurement variables (C_T, A_T, pH, or f_{CO2}) to determine Ω. As saturation states in the world's oceans continue to decline[1,48] and as shoaling saturation horizons more regularly bring corrosive water (Ω_A < 1) onto continental shelves,[6] simple, labor-saving methods to evaluate saturation states are increasingly valuable to researchers and to natural resource and business (e.g., aquaculture) managers.

An important implication of this work is that previously collected datasets of absorbance ratios for $[CO_3^{2-}]_{spec}$ determinations can be reprocessed. If the spectrophotometer used to collect those data is still available (and has not been re-calibrated), its wavelength offset can be determined and the archived absorbance ratios can be corrected with eq 11 to yield R^0 values for use in eq 8 (with the parameters of eqs 12–14). The result is a $[CO_3^{2-}]_{spec}$ dataset with improved precision and an accuracy that is linked to a NIST standard.

Spectrophotometric carbonate measurements are also amenable to use in situ.[23] Realization of in situ measurement capabilities will require direct, physical chemical

characterization of the temperature and pressure dependencies of the $[CO_3^{2-}]_{spec}$ computational algorithm, including equilibrium constants and molar absorptivities. This capability is especially important because in situ spectrophotometric measurements can be obtained essentially continuously (>1 measurement per second), thus allowing for observations of $[CO_3^{2-}]_{spec}$ and saturation state with very high spatial and temporal resolution on moorings, profiling floats, gliders, Niskin rosette frames, seawater flow-through systems, and other platforms.

3.9 Procedural overview

The general procedure to spectrophotometrically measure seawater carbonate ion concentrations is as follows:

First, for a given spectrophotometer, the wavelength offset ($\Delta\lambda_{241.1}$) is determined using SRM 2034[38] from NIST. It is important that this $\Delta\lambda_{241.1}$ value be thereafter associated with all $[CO_3^{2-}]_{spec}$ absorbance data collected with this instrument. If the instrument is recalibrated, the wavelength offset must be redetermined.

Next, $[CO_3^{2-}]_{spec}$ of seawater samples can be determined via the following steps: (1) for each sample, measure an absorbance ratio (R) using absorbances measured at 234, 250, and 350 nm according to the $Pb(ClO_4)_2$ procedure outlined in Section 2.2 and in Patsavas et al.[25]; (2) calculate corrected absorbance ratios (R^0) with eq 11, using the instrument-specific $\Delta\lambda_{241.1}$; and (3) calculate $[CO_3^{2-}]_{spec}$ with eq 8, using R^0 and the salinity-dependent parameters given in eqs 12–14. It is important to note that the titrant-induced perturbation equation presented in Patsavas et al.[25] is not utilized in this updated method.

Additionally, because of the possible use of multi-wavelength measurement techniques[49–51] in the future, we recommend also recording Pb(II) absorbances at wavelengths surrounding the primary target wavelengths (e.g., 233, 234, and 235 nm).

Before being discarded, lead-enriched seawater should be passed through an ion exchange resin (e.g., Chelex® 100 Resin from Bio-Rad) or treated by other means to remove Pb(II), which is toxic to aquatic life.[52–54]

Supporting Information

Figure included to show station locations for the GOMECC-2 and WCOA 2016 cruises. The transect featured in Figure 6 is designated.

Acknowledgements

This material is based on work supported by the National Science Foundation, Award No. OCE-1220110. Support for J.D. Sharp was provided by the NSF Graduate Research Fellowship Program, Award No. 1144244, and by the Anne and Werner Von Rosenstiel Fellowship in Marine Science from the University of South Florida College of Marine Science. Drs. Rik Wanninkhof, Richard Feely, Simone Alin, and their staff, as well as the GOMECC-2 and WCOA 2016 cruises, were supported by NOAA's Ocean Acidification Program, Atlantic Oceanographic and Meteorological Laboratory, and Pacific Marine Environmental Laboratory. We would like to thank Nora Katie Douglas, Dr. Regina Easley, Dr. Mark Patsavas, Dr. Bo Yang, and Dr. Yong-Rae Kim for their assistance in collecting and analyzing field samples. We thank Dana Greeley and Julian Herndon, along with the captain, officers, and crew of the NOAA Ship *Ronald H. Brown*, for support with planning and

execution of the fieldwork. Special thanks are given to Dr. Tonya Clayton for her insightful comments and editorial assistance. This is PMEL contribution number 4644.

References

(1) Feely, R. A.; Sabine, C. L.; Lee, K.; Berelson, W.; Kleypas, J.; Fabry, V. J.; Millero, F. J. Impact of anthropogenic CO_2 on the $CaCO_3$ system in the oceans. *Science* **2004,** *305* (5682), 362–366.

(2) Sabine, C. L.; Feely, R. A.; Gruber, N.; Key, R. M.; Lee, K.; Bullister, J. L.; Wanninkhof, R.; Wong, C. S.; Wallace, D. W. R.; Tilbrook, B.; Millero, F. J.; Peng, T.-H.; Kozyr, A.; Ono, T.; Rios, A. F. The oceanic sink for anthropogenic CO_2. *Science* **2004,** *305* (5682), 367–371.

(3) Doney, S. C.; Fabry, V. J.; Feely, R. A.; Kleypas, J. A. Ocean acidification: The other CO_2 problem. *Annu. Rev. Mar. Sci.* **2009,** *1*, 169–192.

(4) Byrne, R. H. Measuring Ocean Acidification: New Technology for a New Era of Ocean Chemistry. *Environ. Sci. Technol.* **2014,** *48* (10), 5352–5360.

(5) Talley, L. D.; Feely, R. A.; Sloyan, B. M.; Wanninkhof, R.; Baringer, M. O.; Bullister, J. L.; Carlson, C. A.; Doney, S. C.; Fine, R. A.; Firing, E.; Gruber, N.; Hansell, D. A.; Ishii, M.; Johnson, G. C.; Katsumata, K.; Key, R. M.; Kramp, M.; Langdon, C.; Macdonald, A. M.; Mathis, J. T.; McDonagh, E. L.; Mecking, S.; Millero, F. J.; Mordy, C. W.; Nakano, T.; Sabine, C. L.; Smethie, W. M.; Swift, J. H.; Tanhua, T.; Thurnherr, A. M.; Warner, M. J.; Zhang, J.-Z. Changes in Ocean Heat, Carbon Content, and Ventilation: A Review of the First Decade of GO-SHIP Global Repeat Hydrography. *Annu. Rev. Mar. Sci.* **2016,** *8*, 185–215.

(6) Feely, R. A.; Sabine, C. L.; Hernandez-Ayon, J. M.; Ianson, D.; Hales, B. Evidence for upwelling of corrosive "acidified" water onto the continental shelf. *Science* **2008,** *320* (5882), 1490–1492.

(7) Wei, G.; McCulloch, M. T.; Mortimer, G.; Deng, W.; Xie, L. Evidence for ocean acidification in the Great Barrier Reef of Australia. *Geochim. Cosmochim. Acta* **2009,** *73* (8), 2332–2346.

(8) Barton, A.; Hales, B.; Waldbusser, G. G.; Langdon, C.; Feely, R. A. The Pacific oyster, *Crassostrea gigas*, shows negative correlation to naturally elevated carbon dioxide levels: Implications for near-term ocean acidification effects. *Limnol. Oceanogr.* **2012,** *57* (3), 698–710.

(9) Gruber, N.; Hauri, C.; Lachkar, Z.; Loher, D.; Frölicher, T. L.; Plattner, G.-K. Rapid Progression of Ocean Acidification in the California Current System. *Nature* **2012,** *337* (6091), 220–223.

(10) Wanninkhof, R.; Barbero, L.; Byrne, R.; Cai, W.-J.; Huang, W.-J.; Zhang, J.-Z.; Baringer, M.; Langdon, C. Ocean acidification along the Gulf Coast and East Coast of the USA. *Cont. Shelf. Res.* **2015,** *98*, 54–71.

(11) Feely, R. A.; Alin, S. R.; Carter, B.; Bednaršek, N.; Hales, B.; Chan, F.; Hill, T. M.; Gaylord, B.; Sanford, E.; Byrne, R. H.; Sabine, C. L.; Greeley, D.; Juranek, L. Chemical and biological

impacts of ocean acidification along the west coast of North America. *Estuar. Coast. Shelf Sci.* **2016,** 183, 260–270.

(12) Dickson, A. G.; Sabine, C. L.; Christian, J. R.; Eds. *Guide to best practices for ocean CO_2 measurements*. PICES Special Publication: Sidney, BC, Canada, 2007; Vol. *3*.

(13) Langdon, C.; Takahashi, T.; Sweeney, C.; Chipman, D.; Goddard, J. Effect of calcium carbonate saturation state on the calcification rate of an experimental coral reef. *Global Biogeochem. Cycles* **2000,** *14* (2), 639–654.

(14) Langdon, C.; Atkinson, M. J. Effect of elevated pCO_2 on photosynthesis and calcification of corals and interactions with seasonal change in temperature/irradiance and nutrient enrichment. *J. Geophys. Res.* **2005,** *110* (C9).

(15) Bednaršek, N.; Feely, R. A.; Reum, J. C. P.; Peterson, B.; Menkel, J.; Alin, S. R.; Hales, B. *Limnacina helicina* shell dissolution as an indicator of declining habitat suitability owing to ocean acidification in the California Current Ecosystem. *Proc. R. Soc. B* **2014,** *281* (1785), 20140123.

(16) Waldbusser, G. G.; Hales, B.; Langdon, C. J.; Haley, B. A.; Schrader, P.; Brunner, E. L.; Gray, M. W.; Miller, C. A.; Gimenez, I. Saturation-state sensitivity of marine bivalve larvae to ocean acidification. *Nat. Clim. Change* **2015,** *5* (3), 273–280.

(17) Bednaršek, N.; Harvey, C. J.; Kaplan, I. C.; Feely, R. A.; Možina, J. Pteropods on the edge: Cumulative effects of ocean acidification, warming, and deoxygenation. *Prog. Oceanogr.* **2016,** 145, 1–24.

(18) Waldbusser, G. G.; Hales, B.; Haley, B. A. Calcium carbonate saturation state: on myths and this or that stories. *ICES J. Mar. Sci.* **2016,** *73* (3), 563–568.

(19) Keir, R. S. The dissolution kinetics of biogenic calcium carbonates in seawater. *Geochim. Cosmochim. Acta* **1980,** *44* (2), 241–252.

(20) Subhas, A. V.; Rollins, N. E.; Berelson, W. M.; Dong, S., Erez, J.; Adkins, J. F. A novel determination of calcite dissolution kinetics in seawater. *Geochim. Cosmochim. Acta* **2015,** *170*, 51–68.

(21) Morse, J. W. Dissolution kinetics of calcium carbonate in sea water; VI, The near-equilibrium dissolution kinetics of calcium carbonate-rich deep sea sediments. *Am. J. Sci.* **1978,** *278* (3), 344–355.

(22) Morse, J. W.; Arvidson, R. S. The dissolution kinetics of major sedimentary carbonate minerals. *Earth-Sci. Rev.* **2002,** *58* (1), 51–84.

(23) Byrne, R. H.; Yao, W. Procedures for measurement of carbonate ion concentrations in seawater by direct spectrophotometric observations of Pb(II) complexation. *Mar. Chem.* **2008,** *112* (1), 128–135.

(24) Easley, R. A.; Patsavas, M. C.; Byrne, R. H.; Liu, X.; Feely, R. A.; Mathis, J. T. Spectrophotometric Measurement of Calcium Carbonate Saturation States in Seawater. *Environ. Sci. Technol.* **2013,** *47* (3), 1468–1477.

(25) Patsavas, M. C.; Byrne, R. H.; Yang, B.; Easley, R. A.; Wanninkhof, R.; Liu, X. Procedures for direct spectrophotometric determination of carbonate ion concentrations: Measurements in US Gulf of Mexico and East Coast waters. *Mar. Chem.* **2015,** *168*, 80–85.

(26) Fajar, N. M.; García-Ibáñez, M. I.; SanLeón-Bartolomé, H.; Álvarez, M.; Pérez, F. F. Spectrophotometric Measurements of the Carbonate Ion Concentration: Aragonite Saturation States in the Mediterranean Sea and Atlantic Ocean. *Environ. Sci. Technol.* **2015,** *49* (19), 11679–11687.

(27) Byrne, R. H. Inorganic lead complexation in natural seawater determined by UV spectroscopy. *Nature* **1981,** *290* (5806), 487–489.

(28) Soli, A. L.; Stewart, Z. I.; Byrne, R. H. The influence of temperature on $PbCO_3^0$ formation in seawater. *Mar. Chem.* **2008,** *110* (1), 1–6.

(29) Clayton, T. D.; Byrne, R. H. Spectrophotometric seawater pH measurements: total hydrogen ion concentration scale calibration of m-cresol purple and at-sea results. *Deep-Sea Res., Part A.* **1993,** *40* (10), 2115–2129.

(30) Liu, X.; Patsavas, M. C.; Byrne, R. H. Purification and Characterization of meta-Cresol Purple for Spectrophotometric Seawater pH Measurements. *Environ. Sci. Technol.* **2011,** *45* (11), 4862–4868.

(31) Wanninkhof, R.; Zhang, J.-Z.; Baringer, M.; Langdon, C.; Cai, W.-J.; Salisbury, J.; Byrne, R. H. *Carbon dioxide and hydrographic measurements during the* R/V Ronald H. Brown *GOMECC-2 Cruise (July 21 – August 13, 2012)*. Carbon Dioxide Information Analysis Center, Oak Ridge National Laboratory, US Department of Energy: Oak Ridge, TN, 2012. doi: 10.3334/CDIAC/OTG.COASTAL_GOMECC2

(32) Johnson, K. M.; King, A. E.; Sieburth, J. M. Coulometric TCO_2 analyses for marine studies; an introduction. *Mar. Chem.* **1985,** *16* (1), 61–82.

(33) Pierrot, D.; Lewis, E.; Wallace, D. W. R. *MS Excel program developed for CO_2 system calculations*. Carbon Dioxide Information Analysis Center, Oak Ridge National Laboratory, U.S. Department of Energy: Oak Ridge, TN, 2006.

(34) Lueker, T. J.; Dickson, A. G.; Keeling, C. D. Ocean pCO_2 calculated from dissolved inorganic carbon, alkalinity, and equations for K_1 and K_2: validation based on laboratory measurements of CO_2 in gas and seawater at equilibrium. *Mar. Chem.* **2000,** *70* (1), 105–119.

(35) Dickson, A. G. Standard potential of the reaction: $AgCl_{(s)} + 12H_{2(g)} = Ag_{(s)} + HCl_{(aq)}$, and the standard acidity constant of the ion HSO_4^- in synthetic sea water from 273.15 to 318.15 K. *J. Chem. Thermodyn.* **1990,** *22* (2), 113–127.

(36) Lee, K.; Kim, T.-W.; Byrne, R. H.; Millero, F. J.; Feely, R. A.; Liu, Y.-M. The universal ratio of boron to chlorinity for the North Pacific and North Atlantic oceans. *Geochim. Cosmochim. Acta* **2010,** *74* (6), 1801–1811.

(37) Swift, J. H. *A Guide to Submitting CTD/Hydrographic/Tracer Data and Associated Documentation to the CLIVAR and Carbon Hydrographic Data Office*. Scripps Institution of Oceanography, University of California: San Diego, CA, 2008.

(38) Travis, J. C.; Acosta, J. C.; Andor, G.; Bastie, J.; Blattner, P.; Chunnilall, C. J.; Crosson, S. C.; Duewer, D. L.; Early, E. A.; Hengstberger, F.; Kim, C.-S.; Liedquist, L.; Manoocheri, F.; Mercader, F.; Monard, L. A. G.; Nevas, S.; Mito, A.; Nilsson, M.; Noël, M.; Rodriguez, A. C.; Ruíz, A.; Schirmacher, A.; Smith, M. V.; Valencia, G.; van Tonder, N.; Zwinkels, J. Intrinsic Wavelength Standard Absorption Bands in Holmium Oxide Solution for UV/visible Molecular Absorption Spectrophotometry. *J. Phys. Chem. Ref. Data* **2005,** *34* (1), 41–56.

(39) Millero, F. J. The thermodynamics of the carbonate system in seawater. *Geochim. Cosmochim. Acta* **1979,** *43* (10), 1651–1661.

(40) Millero, F. J. Thermodynamics of the carbon dioxide system in the oceans. *Geochim. Cosmochim. Acta* **1995,** *59* (4), 661–677.

(41) Millero, F. J.; Feistel, R.; Wright, D. G.; McDougall, T. J. The composition of Standard Seawater and the definition of the Reference-Composition Salinity Scale. *Deep Sea Res.* **2007,** *55* (1), 50–72.

(42) Mucci, A. The solubility of calcite and aragonite in seawater at various salinities, temperatures, and one atmosphere total pressure. *Am. J. Sci.* **1983,** *283* (7), 780–799.

(43) Venable, W. H., Jr.; Eckerle, K. L. *Didymium Glass Filters for Calibrating the Wavelength Scale of Spectrophotometers – SRM 2009, 2010, 2013, and 2014.* NBS Special Publication 260-66; U.S. Department of Commerce, U.S. Government Printing Office: Washington DC, 1979.

(44) Byrne, R. H.; Breland, J. A. High precision multiwavelength pH determinations in seawater using cresol red. *Deep Sea Res.* **1989,** *36* (5), 803–810.

(45) Newton, J. A.; Feely, R. A.; Jewett, E. B.; Williamson, P.; Mathis, J. Global ocean acidification observing network: Requirements and governance plan. GOA-ON, 2014. http://www.goa-on. org/docs/GOA-ON_plan_print.pdf.

(46) Patsavas, M. C.; Byrne, R. H.; Wanninkhof, R.; Feely, R. A.; Cai, W.-J. Internal consistency of marine carbonate system measurements and assessments of aragonite saturation state: Insights from two U.S. coastal cruises. *Mar. Chem.* **2015,** *176*, 9–20.

(47) Hoppe, C. J. M.; Langer, G.; Rokitta, S. D.; Wolf-Gladrow, D. A.; Rost, B. Implications of observed inconsistencies in carbonate chemistry measurements for ocean acidification studies. *Biogeosciences* **2012,** *9* (7), 2401–2405.

(48) Feely, R. A.; Sabine, C. L.; Byrne, R. H.; Millero, F. J.; Dickson, A. G.; Wanninkhof, R.; Murata, A.; Miller, L. A.; Greeley, D. Decadal changes in the aragonite and calcite saturation state of the Pacific Ocean. *Global Biogeochem. Cycles* **2012,** *26* (3), GB3001.

(49) Byrne, R. H.; Kester, D. R. Ultraviolet Spectroscopic Study of Ferric Hydroxide Complexation. *J. Sol. Chem.* **1978,** *7* (5), 373–383.

(50) Byrne, R. H.; Kester, D. R. Ultraviolet Spectroscopic Study of Ferric Equilibria at High Chloride Concentrations. *J. Sol. Chem.* **1981,** *10* (1), 51–67.

(51) Byrne, R. H.; Young, R. W.; Miller, W. L. Lead Chloride Complexation Using Ultraviolet Molar Absorptivity Characteristics. *J. Sol. Chem.* **1981,** *10* (4), 243–251.

(52) Warnau, M.; Pagano, G. Developmental Toxicity of PbCl2 in the Echinoid *Paracentrotus lividus* (Echinodermata). *Bull. Environ. Contam. Toxicol*. **1994,** *53* (3), 434–441.

(53) Fernández, N.; Beiras, R. Combined Toxicity of Dissolved Mercury with Copper, Lead and Cadmium on Embryogenesis and Early Larval Growth of the *Paracentrotus lividus* Sea-Urchin. *Ecotoxicology* **2000,** *10* (5), 263–271.

(54) Nadella, S. R.; Tellis, M.; Diamond, R.; Smith, S.; Bianchini, A.; Wood, C. M. Toxicity of lead and zinc to developing mussel and sea urchin embryos: Critical tissue residues and effects of dissolved organic matter and salinity. *Comp. Biochem. Physiol. C* **2013,** *158* (2), 72–83.

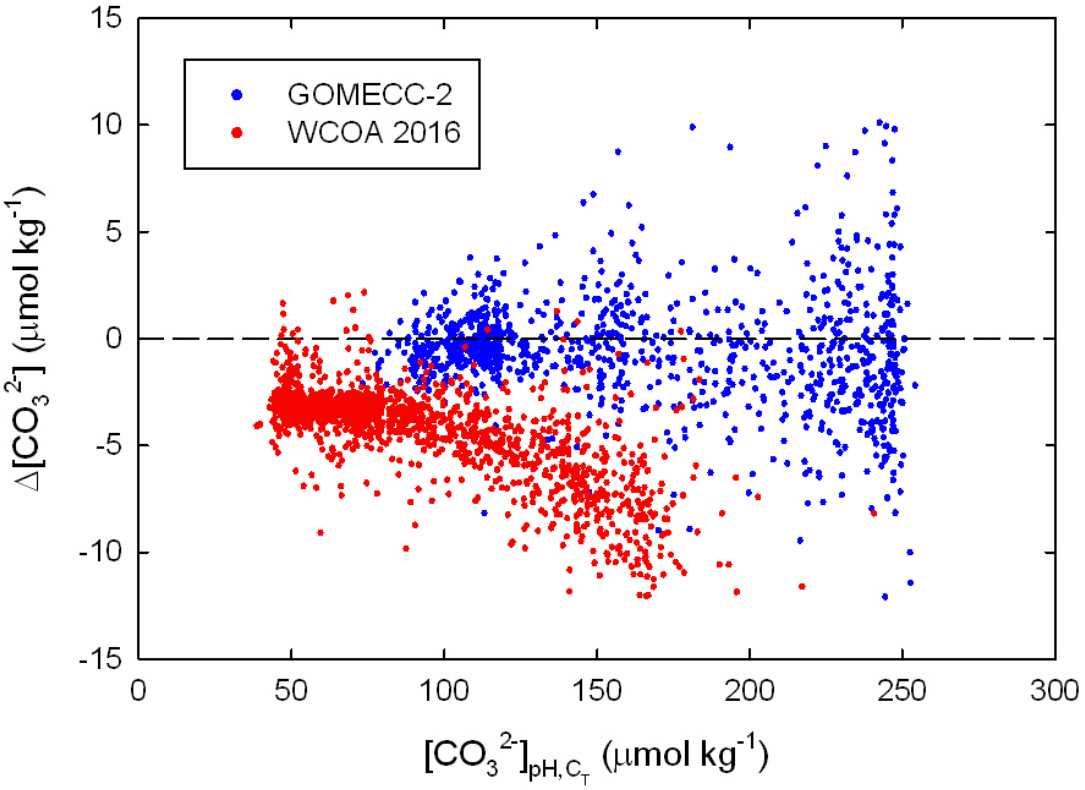

Figure 1. Initial values of $\Delta[CO_3^{2-}]$ (i.e., $[CO_3^{2-}]_{pH,C_T} - [CO_3^{2-}]_{spec}$) from the two NOAA cruises, based on values of *R* and the algorithm of Patsavas et al.[25] Values of $[CO_3^{2-}]_{spec}$ were determined from shipboard absorbance measurements, and values of $[CO_3^{2-}]_{pH,C_T}$ were calculated from paired shipboard measurements of pH_T and C_T.

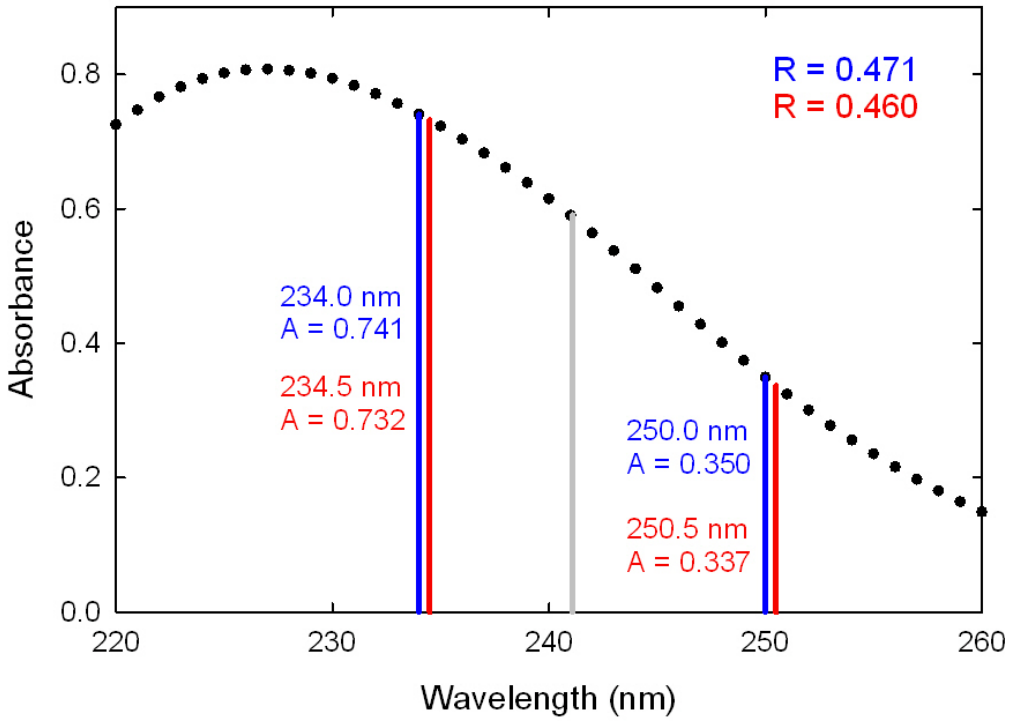

Figure 2. Illustration of how a spectrophotometer with a wavelength offset ($\Delta\lambda_{241.1}$) of only 0.5 nm can produce a significantly different absorbance ratio than a "perfectly calibrated" spectrophotometer. The black dots represent a typical absorbance spectrum observed in seawater enriched with $Pb(ClO_4)_2$. The blue lines represent absorbances measured at 234.0 and 250.0 nanometers (by the "perfectly calibrated" spectrophotometer), and the red lines represent absorbances ostensibly measured at the same wavelengths but actually measured at 234.5 and 250.5 nanometers (by the spectrophotometer with the wavelength offset). The gray line represents the location at which the wavelength offset is assessed according to the NIST standard (241.10 nm). The absorbance ratios calculated using each pair of absorbance measurements are shown.

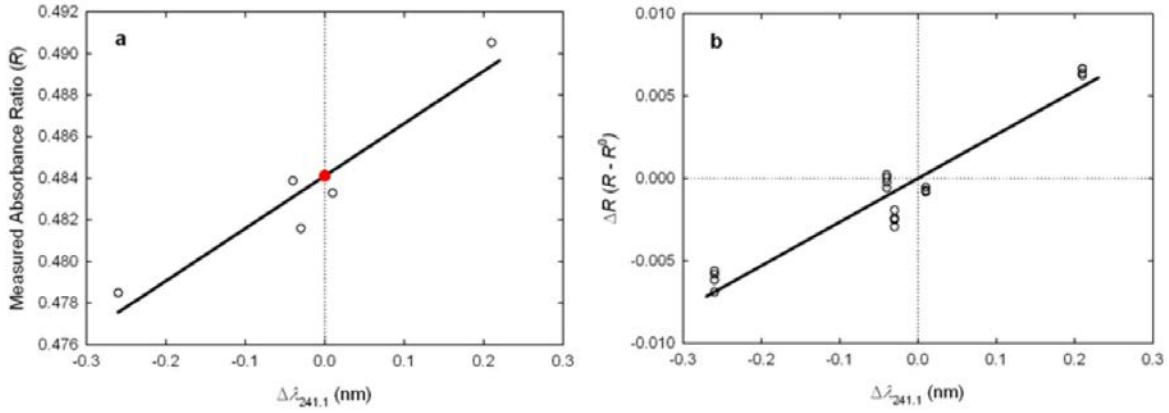

Figure 3. a) Determination of R^0 (absorbance ratio when $\Delta\lambda_{241.1} = 0$) for one of the four seawater batches. R values determined on the five different spectrophotometers are plotted against each instrument's wavelength offset ($\Delta\lambda_{241.1}$). The y-intercept (denoted by the red dot) is the batch-specific R^0 — the absorbance ratio that would have been reported by a "perfectly calibrated" spectrophotometer. b) Determination of the wavelength offset correction equation (eq 11). Values of ΔR ($R - R^0$) were plotted against the wavelength offset of the measuring spectrophotometer. The linear regression yields a correction equation that can be used to convert measured R values to offset-corrected values of R^0.

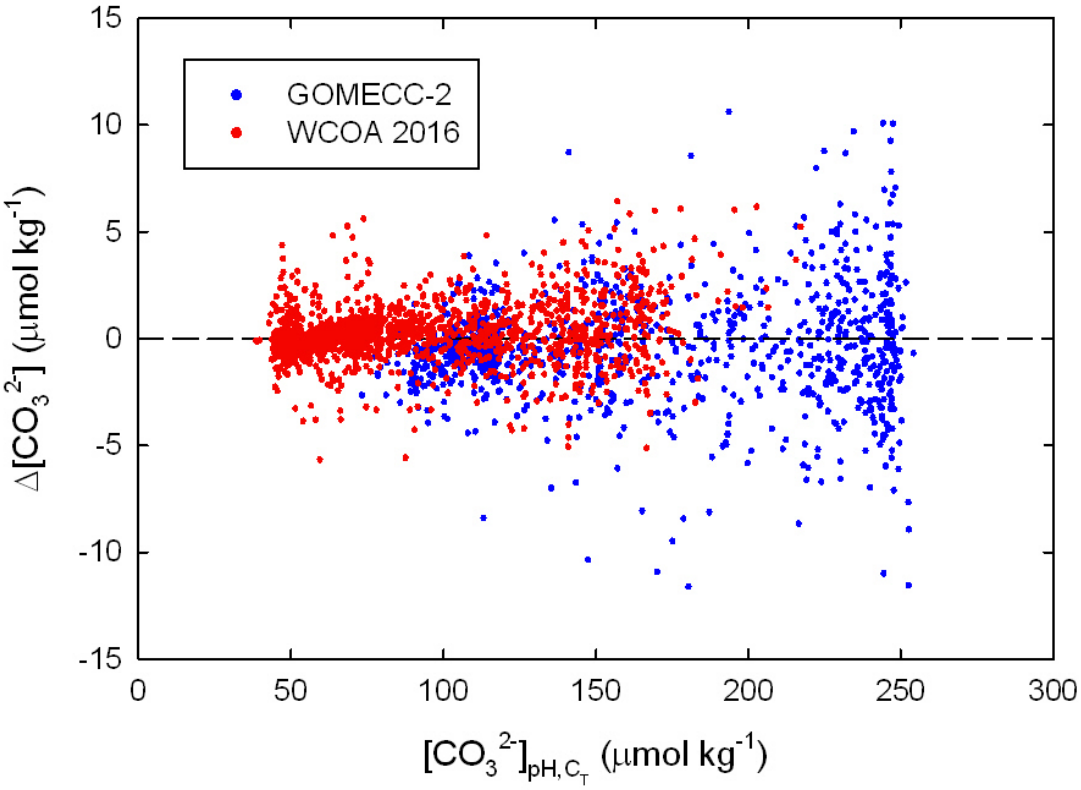

Figure 4. Reprocessed values of $\Delta[CO_3^{2-}]$ (i.e., $[CO_3^{2-}]_{pH,C_T} - [CO_3^{2-}]_{spec}$) from the two NOAA cruises, based on values of R^0 (obtained from eq 11) and the refined $[CO_3^{2-}]_{spec}$ algorithm of this work (eq 8, with the parameters of eqs 12–14). Values of $[CO_3^{2-}]_{spec}$ were determined from shipboard absorbance measurements, and values of $[CO_3^{2-}]_{pH,C_T}$ were calculated from paired shipboard measurements of pH_T and C_T.

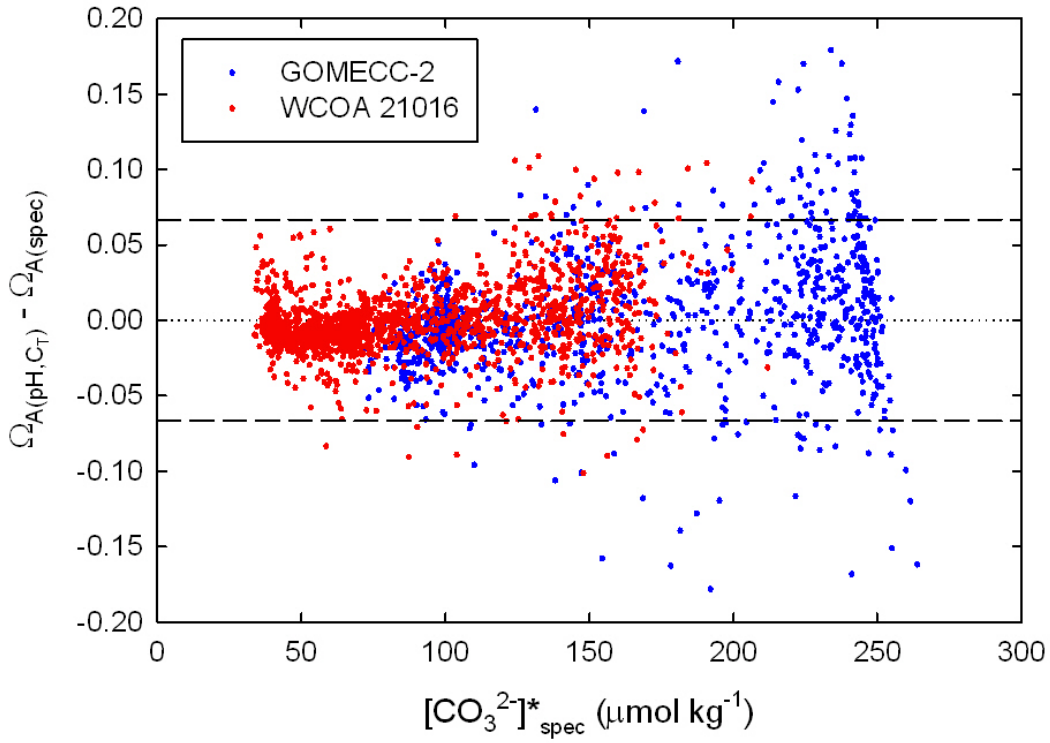

Figure 5. Differences between the two characterizations of in situ aragonite saturation states from the two cruises. Values of $\Omega_{A(pH,C_T)}$ were calculated using paired shipboard measurements of pH_T and C_T, and values of $\Omega_{A(spec)}$ were calculated using shipboard measurements of $[CO_3^{2-}]_{spec}$. The interval constrained by the dashed lines contains 95% of all observations.

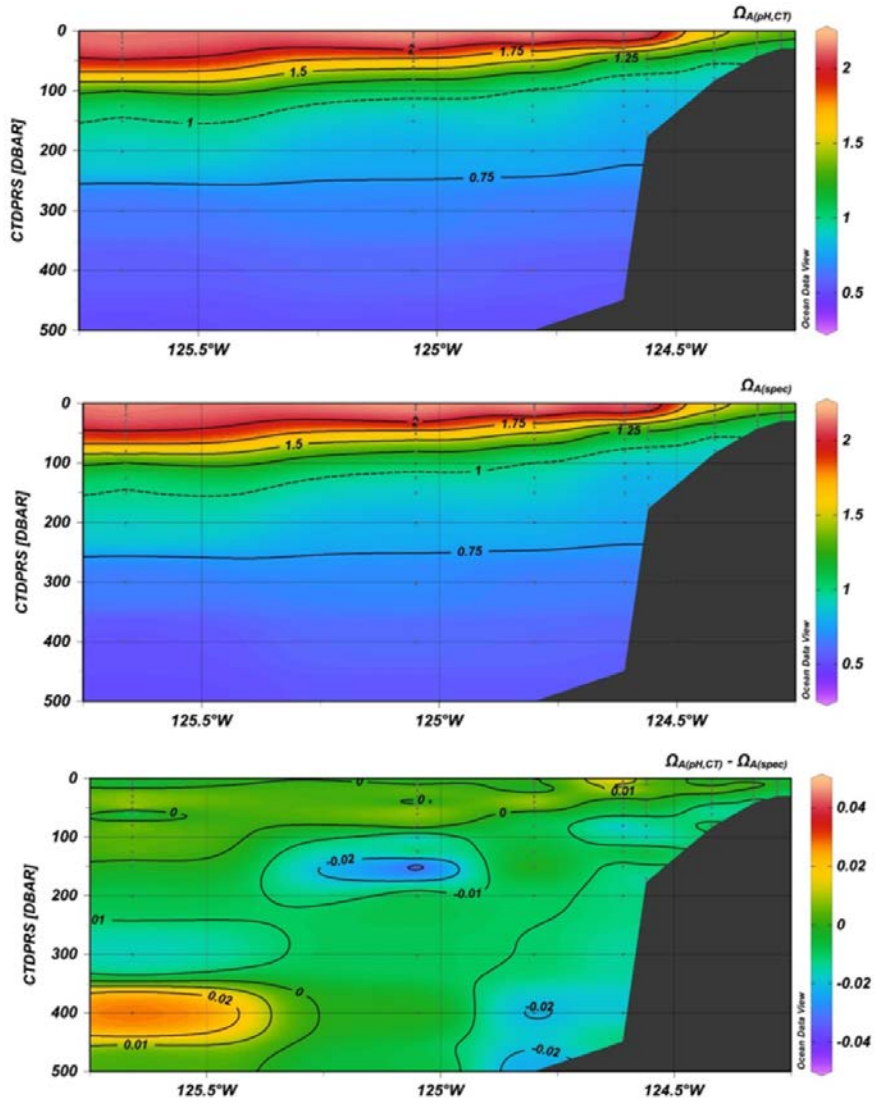

Figure 6. Cross-sections of aragonite saturation state along WCOA 2016 Line 9, near the California/Oregon border (see Figure S1 for location). The top panel shows $\Omega_{A(pH,C_T)}$, determined by calculation from shipboard measurements of pH_T (spectrophotometric) and C_T (coulometric). The middle panel shows $\Omega_{A(spec)}$, determined by calculation from shipboard measurements of $[CO_3^{2-}]_{spec}$, eq 9, eqs 15–17, and eq 10. The dashed lines indicate the aragonite saturation horizon (i.e., where $\Omega_A = 1$). The bottom panel shows the difference between $\Omega_{A(pH,C_T)}$ and $\Omega_{A(spec)}$. On the *y*-axes, *CTDPRS* is pressure in decibars (*DBAR*), as measured by the CTD.

Table 1. Uncorrected and corrected absorbance ratios (R and R^0) for the four different seawater batches, as measured on the five spectrophotometers. The corresponding values of $[CO_3^{2-}]_{spec}$ and $[CO_3^{2-}]_{spec}$ residuals (i.e., measured $[CO_3^{2-}]_{spec}$ minus the $[CO_3^{2-}]_{spec}$ mean for the batch) are also shown. SS_{total} is the total sum of squared residuals. These data were all processed using the algorithm of Patsavas et al.[25]

Seawater Batch #	R	$[CO_3^{2-}]_{spec}$ (µmol kg^{-1})	$[CO_3^{2-}]_{spec}$ Residual (µmol kg^{-1})	R^0	$[CO_3^{2-}]_{spec}$ (µmol kg^{-1})	$[CO_3^{2-}]_{spec}$ Residual (µmol kg^{-1})
	0.452	245.59	0.13	0.452	246.27	2.58
	0.452	245.20	–0.27	0.454	241.86	–1.84
1	0.447	259.16	13.69	0.454	241.07	–2.62
	0.459	228.72	–16.75	0.453	242.65	–1.04
	0.451	248.67	3.21	0.452	246.62	2.92
	0.483	181.29	0.27	0.483	181.71	1.78
	0.484	180.33	–0.68	0.485	178.65	–1.29
2	0.478	189.26	8.25	0.485	177.95	–1.99
	0.491	170.14	–10.87	0.485	178.62	–1.31
	0.482	184.05	3.04	0.482	182.75	2.81
	0.495	164.12	0.04	0.495	164.49	1.36
	0.496	162.80	–1.27	0.498	160.98	–2.15
3	0.490	171.96	7.89	0.497	162.10	–1.03
	0.503	154.25	–9.83	0.497	161.98	–1.15
	0.493	167.25	3.17	0.494	166.11	2.98
	0.520	132.90	–0.18	0.520	133.18	0.81
	0.521	132.28	–0.80	0.522	131.17	–1.19
4	0.514	139.80	6.73	0.521	132.32	–0.05
	0.528	125.54	–7.54	0.522	131.15	–1.22
	0.519	134.87	1.79	0.519	134.02	1.65
		SS_{total} =	**951.0**		**SS_{total} =**	**68.9**